

SAE Paper Number 2019-01-2356 ©2019 Society of Automotive Engineers International. This paper is posted on this website with permission from SAE International. As a user of this website you are permitted to view this paper on-line and print one copy of this paper for your use only. This paper may not be copied, distributed or forwarded without permission from SAE.

# The Investigation of the Structure and Origins of Gasoline Direct Injection (GDI) Deposits.

**J Barker J Reid and S Mulqueen**  
Innospec

**G J Langley and E M J Wilmot**  
University of Southampton

**S Vadodaria**  
University of Warwick

**J Castle**  
University of Sheffield

**J Whitaker**  
University of York

Copyright © 2019 SAE Japan and Copyright © 2019 SAE International

## ABSTRACT

The legislative pressures on environmental targets combined with fuel economy requirements have led to the GDI engine enjoying a renaissance. This is because the technology is considered to be the leader in meeting those requirements. However it is also recognized that the engine suffers from injector deposits (ID) and that understanding the formation of and characterization of such deposits is required. This study will deal with the characterization and morphology of injector deposits as well as the fuel constituents leading to such deposits. A number of analytical techniques were used to undertake this such as Scanning Electron microscopy and X-ray Fluorescence (SEM/EDS) mapping with Fourier Transform Infra-red mapping, in conjunction with mass spectrometry studies. Further, work will be described regarding new deposit control additives (DCAs) for GDI which are more effective than traditional DCAs.

## INTRODUCTION

Historically [1] the introduction of direct injection spark ignition (DISI) engines was because of the requirements of the aeronautical industry [2] and may be traced back to the early development of the Leon Levavasseur aviation engine in 1902 [3]. Automotive two stroke versions were introduced in 1952 by Hans Scherenberg [4] and used in the Gutbrud and Goliath

automobiles. The automotive versions of this equipment had problems which limited its take up. Vapour locks and requirements for fuel pump adjustment made them unpopular in relation to the new carburettor based engines. Carburettor based engines remained popular until the early 1980's. The carburettor not only mixed the intake air with the fuel in the correct ratio for the driving conditions it also distributed the mixed air and fuel ratio to the cylinder next in line for the combustion event at the exact time it was needed. This resulted in the combustion charge being sensitive to vapour pressure, fuel composition, and positioning amongst other fuel variables. The consequence was driveability issues and increased exhaust emissions. These in conjunction with the requirement for specific economy and power requirements led the adoption of fuel injection equipment [5,6]. The first systems were known as "throttle body" or "single point" injection systems. The carburettor had served the automotive industry well for over a century but was becoming unwieldy and expensive in its multiple carburettor incarnation of the 1980s. As requirements for higher power outputs were required. It seemed a logical step to combine the technology of fuel injection and the cost advantages of a single carburettor. In the "Throttle Body Injector (TBI) system a carburettor body and a single fuel injector replaced the jets. One injector supplied fuel to all the jets (figure 1).

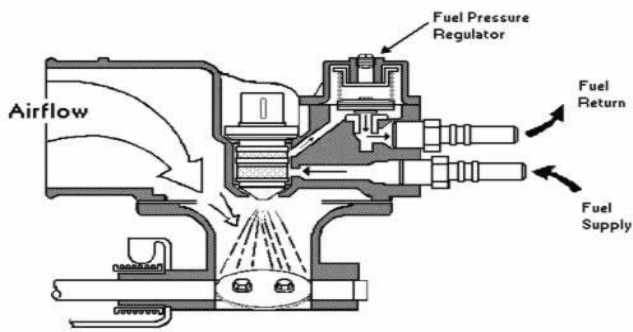


Figure 1 “Throttle Body” (TBI) Fuel Injector System

Even though this injection system provided more control over the amount of fuel injected and injection timing, fuel distribution problems remained. The TBI retained the carburetor characteristic of poor air to fuel ratio matching when moving from cylinder to cylinder and fouling of the injector was found to occur [9]. The emissions legislation at that time was also as usual a major influence in the next development of gasoline injector systems. Legislation saw the introduction of catalyst traps but without accurate air/fuel ratio ( $\lambda$ ) control these vehicles emitted  $H_2S$  under certain driving conditions which resulted in complaints [10]. The adoption of an old idea [6] allowed the next leap in fuel injection design. This was the use of multi-point fuel injection in the fuel intake port itself. These systems were known as Port Fuel Injection (PFI) systems where each cylinder has a dedicated fuel injector, (Figure 2).

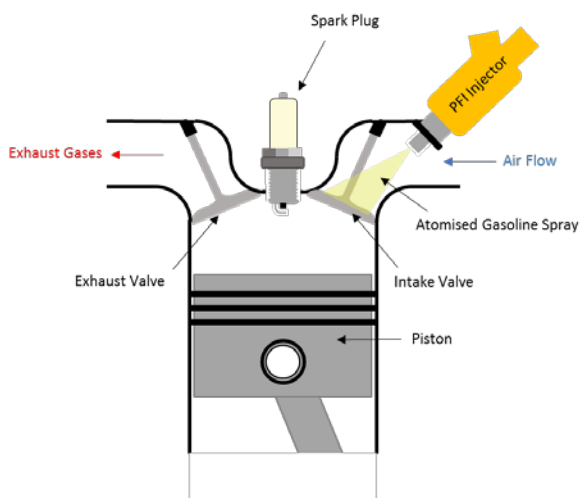


Figure 2 Port Fuel (PFI) System

The ever increasing need to meet global emission regulations and consumer demand for greater fuel efficiencies then led to further fuel injector developments to Gasoline Direct Injector (GDI) systems (Figure 3)

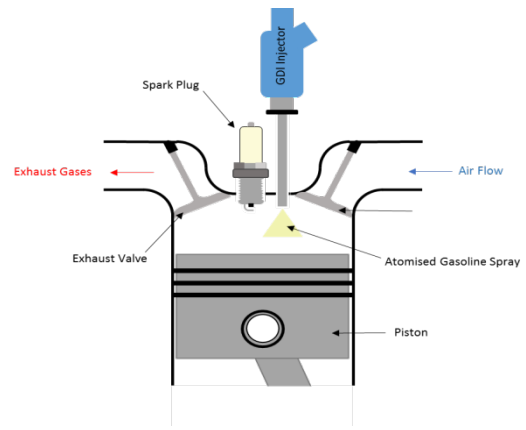


Figure 3 Gasoline Direct Injection (GDI) System

The GDI injector works by highly pressurised gasoline being injected via a common rail fuel line directly into the combustion chamber of each cylinder. The adoption of this technology has been high. For example in the United States between 2008 and 2016 a ~38% increase in market share was seen [11]. In Europe there is a similar trend with 2014 ~35 % market share growth for GDI by 2014 [12]. The reasons for this adoption in detail are increased fuel efficiencies by reducing pumping losses compared to carburettor and PFI engines; a higher power output by reducing mechanical and pumping losses and most importantly more accurately controlled regulated emissions by on board management of fuelling regimes. The improved emissions control being the result of higher fuel pressures which led to to smaller droplet sizes. In detail the GDI system is similar to that of High Speed Direct Injection diesel systems utilising a common rail system to circulate high pressure fuel where the injectors have access to a constant fuel supply. The engine management system fires the injectors at the optimum moment for a specific duration based around the demand and driving conditions experienced. In comparison with PFI GDI injection pressures are in excess of 100 bar compared to 5 bar. Concomitant changes in fuel droplet size are seen from 120-200  $\mu m$  to <20  $\mu m$ . Though GDI technology allows the motor manufacturer to reach emission and fuel economy targets there are also downsides to the technology concerning deposit formation and particulate emissions.

The formation of GDI injector deposits manifests itself in the effect upon fuel trim (Figure 4). For any gasoline fuelled vehicle with a catalytic convertor it is essential that the air fuel ratio of the combustion event is at 14:1; commonly known as Lambda ( $\lambda$ ) 1. The lambda or oxygen sensor monitors the amount of oxygen in the exhaust. At the same time the vehicle computer receives information from a mass air flow sensor (MAF) measuring the mass of air being consumed by the engine and how much fuel is being injected by the injector pulse width i.e. how long the injector is open. The on-board computer summarizes this data and calculates if the engine is running too rich; too much fuel; or too lean; too little fuel and immediately adjusts the injector pulse width (IPW) accordingly. This adjustment is described as short term fuel trim (STFT). This occurs many times a second depending on the drive cycle, altitude and other small changes in engine

and fuelling conditions. The constant variation of the STFT is transferred to the vehicle computer and known as long term fuel trim (LTFT)



Figure 4 Fuel Trim [14]

Injector fouling will be a mechanism for influencing the LTFT of a vehicle. As deposits build up in the injector fuel flow becomes more restricted to compensate the vehicle computer increases the amount of time the injector is open. When the LTFT reaches 25% a vehicle warning light will indicate dealer investigation of the problem is required.

Such field issues seen in Europe have led to the industry response of a proposal for a CEC engine test by Volkswagen, TDGF-113 [12]. At the time of writing the test is in its final development phase. The terms of reference of this new test being: Vehicle manufacturers are increasing the market share of direct injection spark ignited engines (DISI) to meet the demands of legislative regulations and the demands of car drivers. DISI engines offer multiple advantages over common port fuel injection engines (PFI) but they can be susceptible to deposit formation even at the fuel injector nozzle. Fuel injector deposits have been identified as a root cause for a number of negative effects that can impact the normal operating mode of the engine. New exhaust emission legislation may require injector types with a higher dependency on fuel DCA (Deposit Control Additives) performance even for higher mileage. Industry DCA performance tests are solely designed for port fuel injection engines (PFI) with the assessment of IVD (intake valve deposits) and the assessment of deposit formation at port fuel injectors. An extrapolation of PFI engine test results to predict the DCA performance in a DISI-engine is limited due to different ambient conditions (temperature, pressure, combustion gases, and flow behaviour) at the injector tip. For this reason, a new test is required that is able to discriminate between a fuel that produces no significant injector deposits and one which cannot prevent injector fouling and as such is not able to keep the injectors clean enough to run the engine in compliance with the above mentioned requirements. The CEC is not aware of any official engine test procedure to evaluate the effects of DISI injector fouling that is representative of the present and future risks due to injector fouling. Expected goals for the test development are that the test is required to be able to discriminate between a fuel that produces no significant injector deposits and one which cannot prevent injector fouling and could cause drivability issues due to a severe increase of the injection time. Another parameter to reflect potential drivability

issues is A/F ratio (Air/Fuel ratio). A testing tool for gasoline additive performance based on a widely used GDI engine is currently in development to produce a reliable and safe test with good precision. The test should facilitate a practical, adoptable and easily understandable limit setting. A fully qualified CEC test procedure is in development, with the following criteria.. A test must be able to discriminate between calibration fuels of known field performance on the chosen parameters as per CEC requirements. Test repeatability and reproducibility must meet CEC requirements. The timing target for completion of test development must be defined The laboratory chosen to lead the test development must meet CEC quality requirements. The registered office and test benches must be situated in Europe and have experience of running engine tests. The test procedure is performed with new six hole injectors type 03C906603E/F from Bosch or Magneti Marelli. The injector run-in procedure is performed at high load for four hours. The test procedure is a steady state test at an engine speed of 2000rpm and a constant torque of 56Nmm (=5 bar mean effective pressure) and the thermostat is in serial condition. Nozzle coking is measured as a change of injection timing. Due to nozzle coking, the diameter of the injector holes is reduced, and in response the injection time is adjusted by the engine control unit (ECU). The injection time in milliseconds is read directly from the ECU. A linear trend calculation at the start of and at the end of the test defines the nozzle coking during the forty-eight hours of the dirty- up phase. The total nozzle coking after forty eight hours is the reference for the recovery calculation during the twenty-four hours clean-up phase (Figure 5).

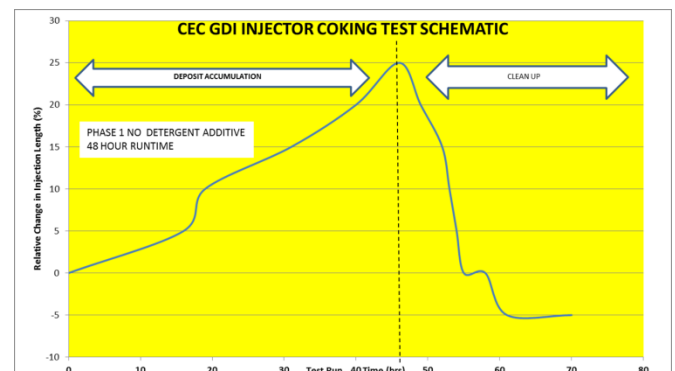


Figure 5 Schematic of the GDI engine test

This test is now in its final development phase

The other problem with GDI is particle emission levels. This occurs because of incomplete fuel volatilization together with higher combustion pressures, partially rich fuel zones and the “wetting” of piston and cylinder surfaces. The majority of emissions occur during cold start and high load conditions and during the warm up phase. This can vary according to load, drive cycle and driver demands.

The deposit and particulate issue is a priority for the industry to understand and manage. It is the purpose of this paper to describe the work done to investigate methods of understanding and ways of mitigating deposit formation.

## INVESTIGATIONS IN GDI DEPOSITS AND THEIR FORMATION.

A selection of linked fuels and injectors from the field and standardized bench engine tests were sourced from the United States of America and Europe. A typical injector is shown below (Figure 6).



Figure 6 Typical GDI injector<sup>15</sup>

### DEPOSITS

The injectors were broken down into their component parts (Figure 7).



Figure 7 Dismantled GDI injector a) core body 1, b) core body 2, c) injector nozzle, d) injector needle, e) pin, f) washer and g) spring.

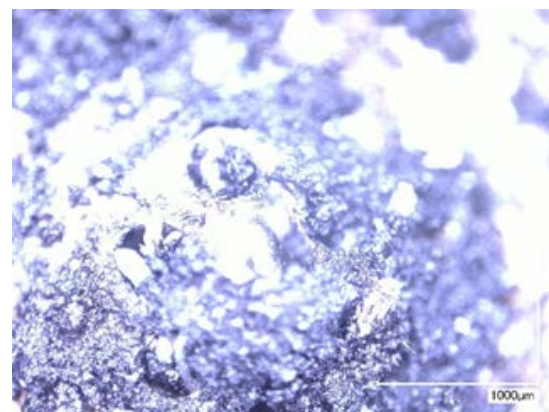
The parts showed both external and internal deposits. In this paper we will concentrate on the deposits in and around the nozzle holes. The other deposits will be the subject of future publications. A simple visual inspection of the injector nozzle can indicate the degree of fouling (Figure 8).



Clean Injector Example



Fouled Injector Example



Fouled Injector Example

Figure 8 Photomicrographs of “Clean” and Fouled Injector Nozzles.

Scanning Electron Microscopy (SEM)/ Energy, Dispersive X-Ray Spectroscopy (EDS)/Fourier Transform Infra-Red Microscopy (FTIRM) Studies

The fouled injectors they were analysed using a Hitachi TM3030Plus SEM with Bruker Quantax EDS and a Nicolet iN10MX microscope. The SEM shows the structure and morphology of the deposits and the EDS the semi-quantitative elemental composition. The infra-red spectroscopy informing with regard to functionality. Two examples will be looked at in detail.

### INJECTOR 1 SEM Analysis:

The nozzle of the injector was heavily fouled, with large aggregations of material being observed (Figure 9). The distribution of deposits was asymmetrical, with deposits accumulated primarily on one side and also on the raised tip, which suffered from a particularly heavy build-up of material. Most of the holes were almost completely obstructed with only two holes visible (Figure 10, and 11). The inner walls of the holes showed fouling and there were also deposits that had formed over the outside of the holes. Deposits with different morphologies were observed on the injector. Most of the surface was covered by a thin film of carbonaceous deposits (Figure 12; D). On top of this, spherical deposits of approximately 60-100  $\mu\text{m}$  in diameter were present (Figure 12; C). These were distributed mainly across the lower flat regions and were usually covered in pores. A prominent deposit with flatter yet rough and uneven surfaces, unlike the other more common deposit structures, was also observed (Figure 12; B). Next to this was a raised deposit (Figure 12; A) that was covered in a multitude of smaller globular structures (Figure 13). Each of these globular structures on the larger deposit were covered in minor round bumps (Figure 14) as observed at higher magnification.

### ELEMENTAL ANALYSIS

The deposits present on injector A consisted predominantly of carbon and oxygen. (Figure 15). Other elements present were calcium, sulfur and silicon. These elements were detected across the whole surface of the injector. Linear EDS scans were used To investigate in more detail how their abundance varied across the injector. This revealed that the concentration of trace elements dropped in the deposits directly around the fuel output holes (figure 16).

The elemental distribution map (Figure 17) indicates that C and O were present in all deposit material. To investigate whether deposits of different physical structures had different chemical compositions, the relative abundances of C and O were examined using localised EDS scans in numerous locations. This revealed that deposit B had a slightly higher proportion of C than deposits B-D, which all contained relatively similar proportions of C and O.

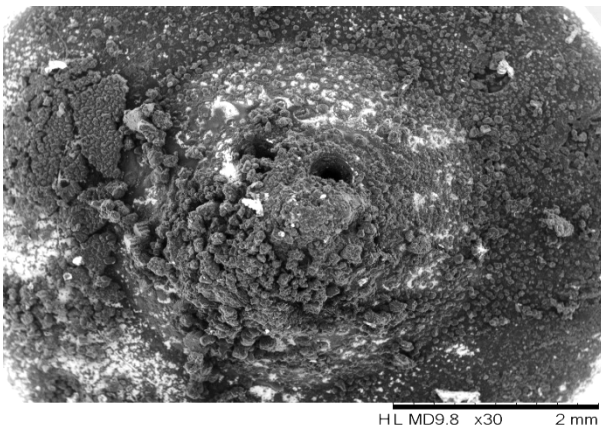


Figure 9. SEM Micrograph of injector 1 nozzle tip



Figure 10. SEM micrograph of hole in injector 1 nozzle

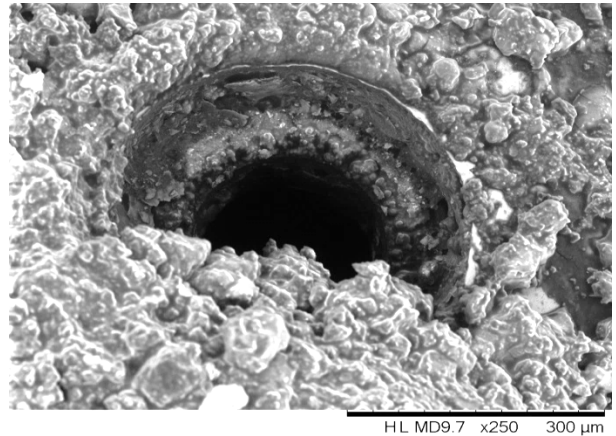


Figure 11. SEM Micrograph of hole in injector 1 nozzle

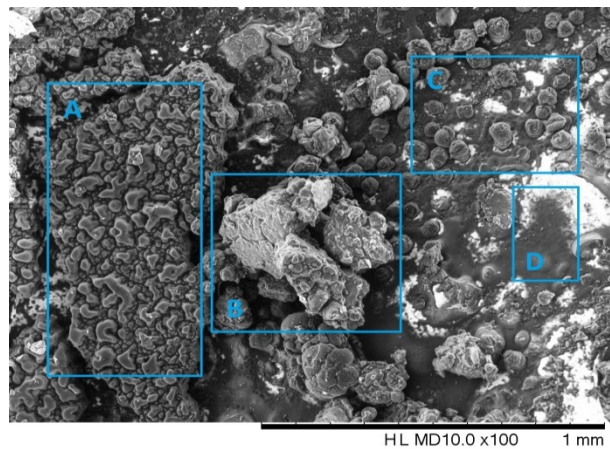


Figure 12. SEM Micrograph of injector 1 deposits

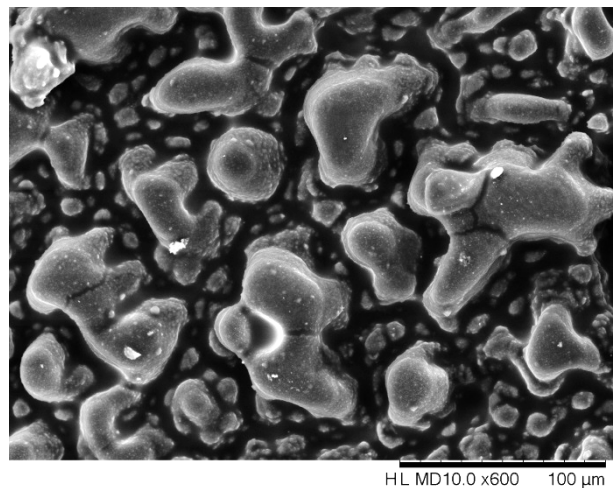


Figure 13. SEM Micrograph of region 1 in figure 12 at higher magnification

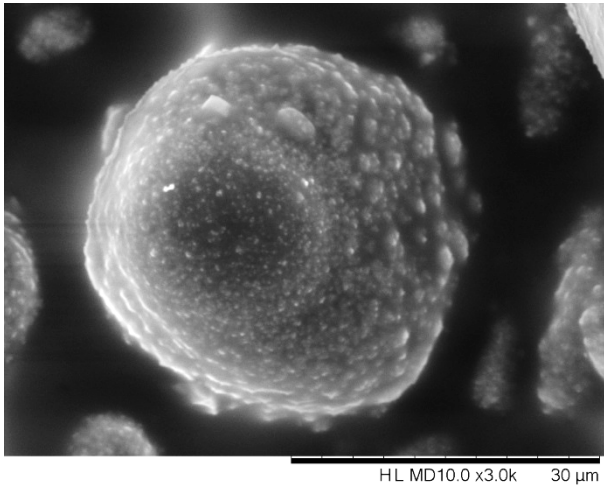


Figure 14. SEM Micrograph of region A in figure 18 at higher magnification

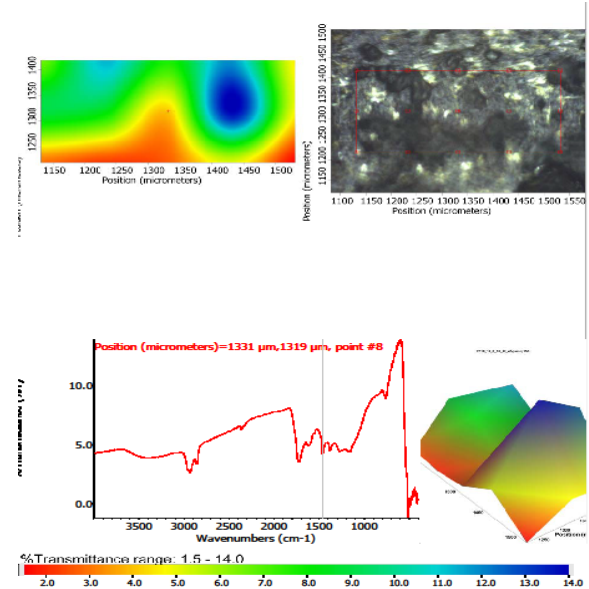


Figure 18 Infra-red Microscopy Map of Injector 1

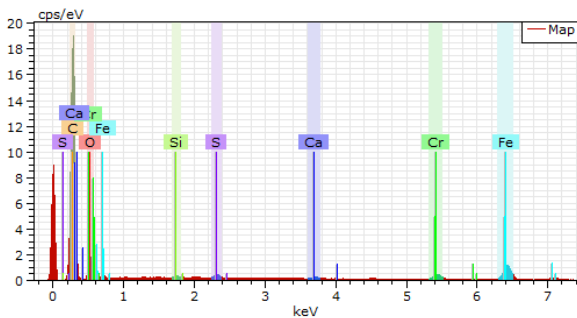


Figure 15. EDS spectrum of injector 1 nozzle tip

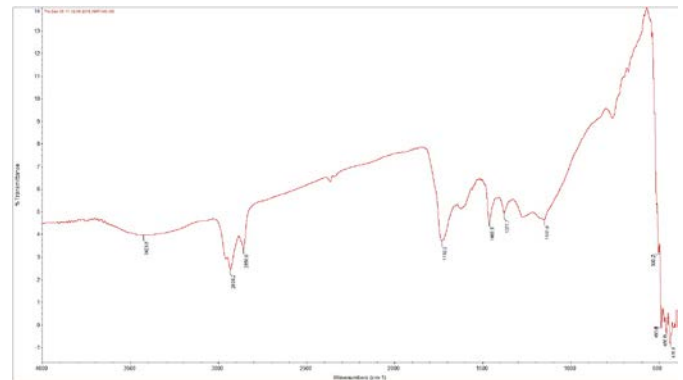


Figure 19 Infra-red Spectrum near Injector 1 Orifice.

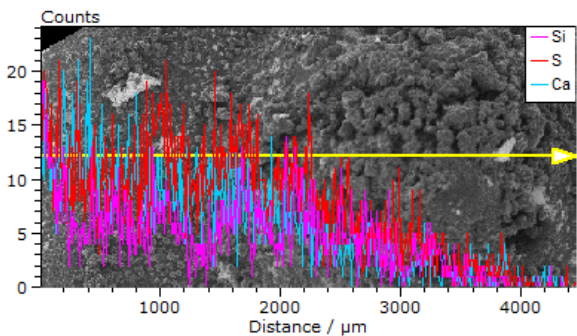


Figure 16. Linear EDS scan for detection of Si, S and Ca across a region of injector 1

The spectra show different responses across the injector surface with blue to red changes showing the chemical distribution is not homogenous. The spectra both in the map and the single spot spectrum (Figures 18-19), show carbon oxygen bond functionality at  $1722\text{cm}^{-1}$  as well as fuel residual hydrocarbons e.g.  $2930\text{cm}^{-1}$ .

### INJECTOR 2 SEM Analysis

Injector 2 showed similarly heavy fouling with a significant build-up of deposits around the raised tip (Figure 20) Injector 2 also had an uneven distribution of deposits, with one side much barer (Figure 21; region A). Its holes were almost completely blocked by deposits formed inside the holes, around the inner walls and around the outside of the orifices (Figures 22-23).

The commonly found spherical deposits were again observed on the lower surface of injector 2. The closer in proximity towards the central tip, the larger in size they became. When observed at higher magnification, deposits of this type were found to have an irregular surface that was covered in small bumps and protrusions, but did not contain pores (Figure 24). There were much thicker accumulations of deposits towards the tip. These also had an irregular surface



Figure 17. Elemental distribution mapping of C, O, Fe, Cr and N on region of injector 1.

### INFRA-RED SPECTROSCOPY

structure, littered with small crystal-like protrusions (Figure 25).

**ELEMENTAL ANALYSIS**

The deposits on injector 2 consisted mostly of carbon and oxygen with traces of sulfur, silicon, calcium and phosphorus (Figure 26). These trace elements were detected across the entire surface of the injector (Figure 27). No correlation was found between location and concentration.

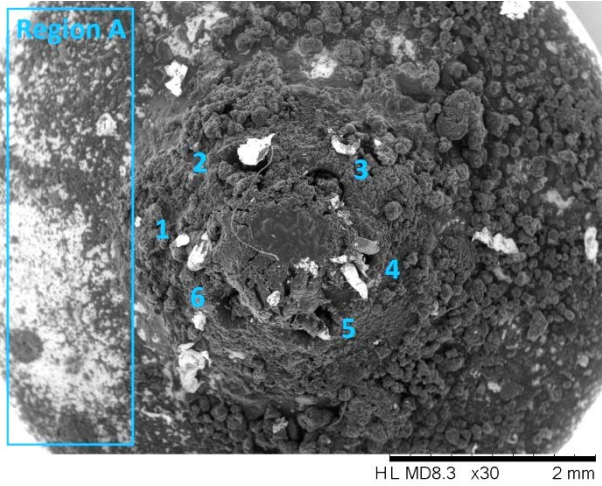


Figure 20. SEM Micrograph of injector 2 nozzle tip

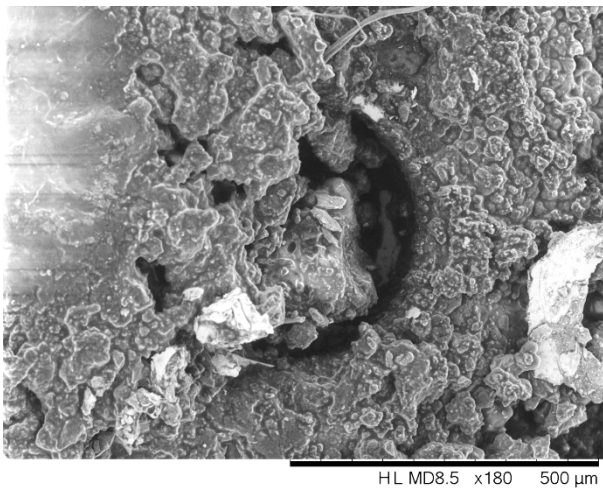


Figure 21. SEM Micrograph of hole 3 in injector 2 nozzle

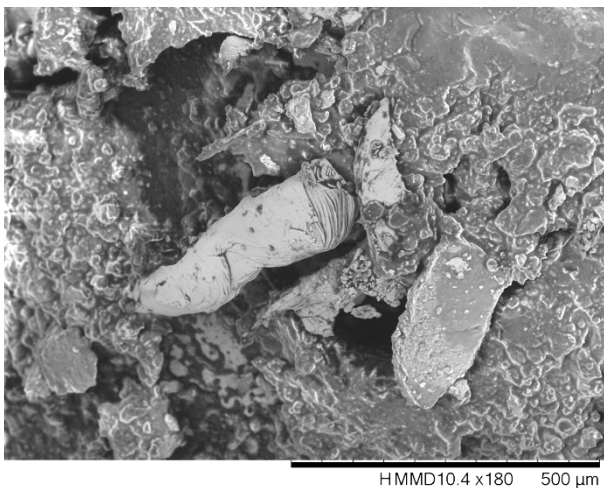


Figure 22. Mixed SEM Micrograph of hole 4 in injector 2 nozzle

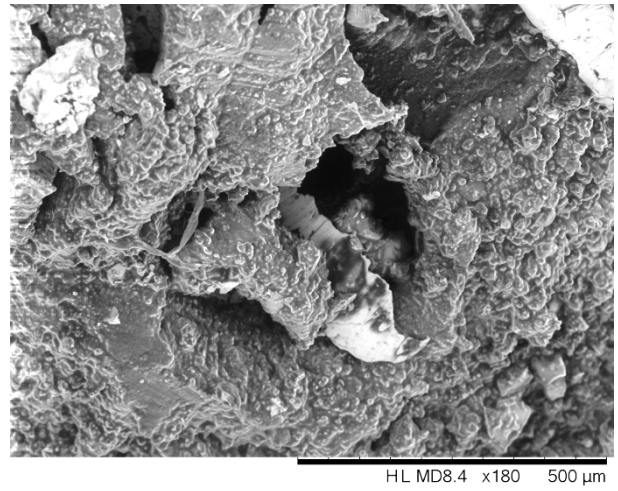


Figure 23. SEM Micrograph of hole 5 in injector 2 nozzle

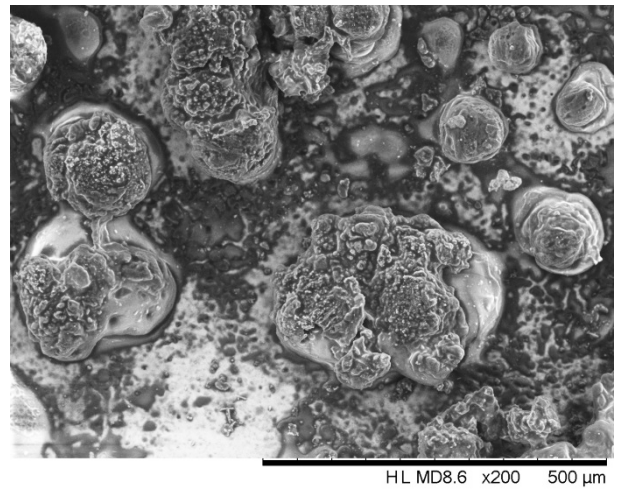


Figure 24. SEM Micrograph injector 2 deposits

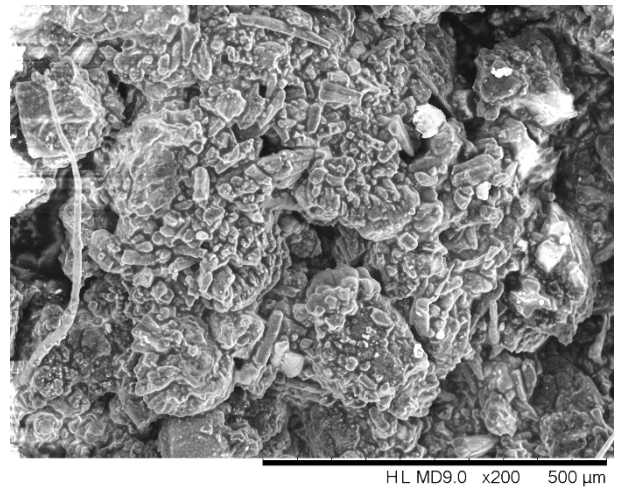


Figure 25. SEM Micrograph of injector 2 deposits

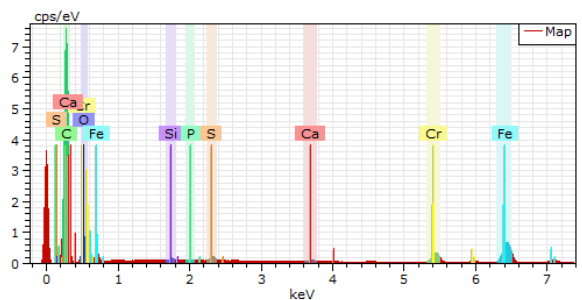


Figure 26. EDS spectrum of injector 2 nozzle tip

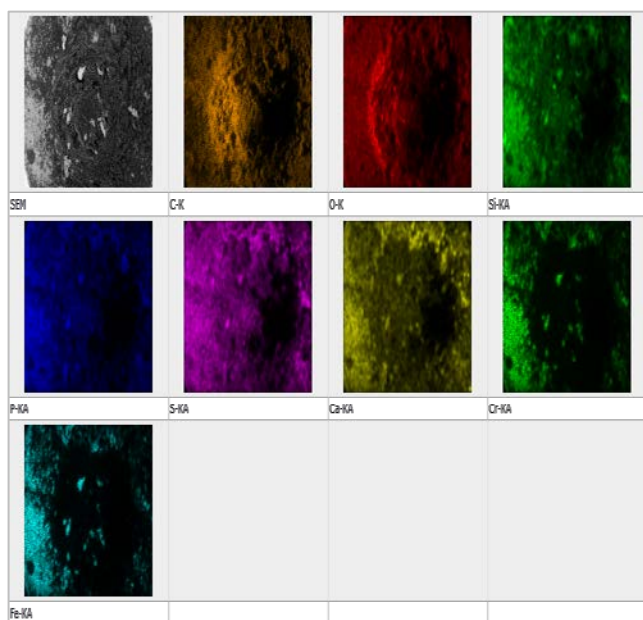


Figure 27 EDS map of injector 2 Surface.

The characterization of the deposits has shown them to be similar to that found by Dearne *et al* [16].

- The nozzle orifices show both internal and external deposits on the injector nozzle.
- The deposits are asymmetrically distributed across the nozzle. This may be a result of proximity to intake or exhaust valves, [17].
- The EDS analysis shows carbon and oxygen as the main constituents of the deposits but also traces of calcium, sulfur and phosphorus indicating lube oil participation in deposit formation.

• The deposits inside the internal orifices of the injectors are formed from liquid fuel directly, as during each injection these channels are flushed with fuel. After injection, a small amount of fuel remains. Contained in this fuel is a dispersion of deposit precursors. These are highly oxidized and polymeric species formed during storage, from the oxidation of unsaturated fuel components *via* a series of complex chain reactions [18-21].

A number of spherical deposits were also noted originating from fuel droplets [22-23]. and flat deposits with adjoining holes. These structures are probably formed by the production of gas bubbles at the surface of a layer of liquid. As the bubbles continue to be generated and subsequently collapse, carbonization of the surface occurs resulting in a flat deposit in the holes [24].

## FUELS

Literature sources have indicated that the presence of certain chemical constituents in gasoline can promote GDI nozzle fouling [25]. Mass spectrometric analyses of the fuels associated with the fouled injectors were developed to investigate any links with the possible “bad actors”.

### Peroxide and olefins:

Literature[19] suggests these compounds play role in the formation of deposits and gums within the fuel injectors. Typical examples of these compounds are

described in Figure 28

NAME	STRUCTURE
dicumyl peroxide	
di-t-butyl peroxide	
1,1-di(t-butylperoxy)-	
3,3,5-trimethylcyclohexane	
Indene	
Isoprene	
Anthracene	
Dicyclopentadiene	

Figure 28 peroxide and diolefin examples found in gasoline

Initial work using gas chromatography-mass spectrometry (GC/MS) showed decomposition of these compounds. Dicumyl peroxide for example produced the decomposition product acetophenone [27] and is likely to be combination of the relatively weak peroxide bond and the elevated temperatures experienced in the GC-MS injector, column, transfer line and/or ionisation source. Changing instrumental conditions did not resolve the decomposition so more sophisticated mass spectrometric techniques were deployed.

Ultra high pressure super critical atmospheric pressure ionization mass spectrometry (UHPSFC-API MS) of peroxides and diolefins.

Positive ion electrospray ionization (ESI) can be used to analyse thermally labile peroxides due to the low thermal energy input into the molecules and subsequent ions during the ionization process. The thermal energy is dissipated by the evaporation of the eluent.

Positive ion atmospheric pressure photo-ionization (APPI) can be used for the detection of diolefins. The same properties that make diolefins (conjugated

double bonds) problematic with respect to deposition within fuel injectors are the same properties that make compounds suitable for ionization by positive ion APPI (*i.e.* presence of  $\pi$ -electron systems). Thus, positive ion APPI can be used to selectively ionize these compounds within fuel samples, highlighting their presence with little interference from the hydrocarbon matrix observed *via* GC-MS techniques. For both the analysis of the peroxides and the diolefins, the API techniques can be interfaced with UHPSFC. UHPSFC is a chromatographic technique which is suitable for the thermally labile peroxides due the low operating temperature, unlike that of GC (Gas-Chromatography), and the good compatibility of the supercritical CO<sub>2</sub> with gasoline, unlike the aqueous phases of reversed-phase HPLC (High Pressure Liquid Chromatography). An example of this type of analysis for dicumyl peroxide (Figure 29), shows this technique does not have the decomposition problems of GC/MS.

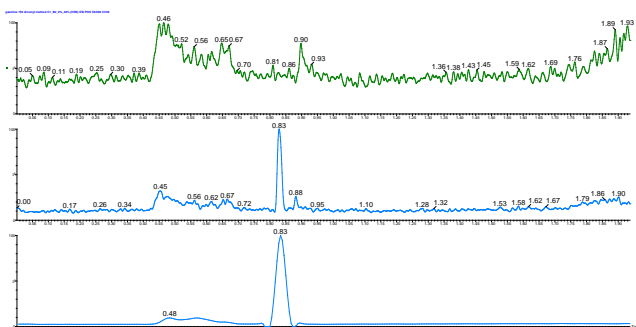


Figure 29 (top) UHPSFC +ve-ESI MS (base peak ion current chromatogram) BPICC of Gasoline used in injector 2. (middle) UHPSFC+ve ESI MS of gasoline used in injector 2 spiked with dicumyl peroxide. (bottom)UHPSFC+ve ESI MS (selected ion recording) SIR for  $m/z$  119 BPICC of gasoline used in injector 2 spiked with dicumyl peroxide.

The diol compounds are also suitable for the UHPSFC analytical approach (Figure 30).

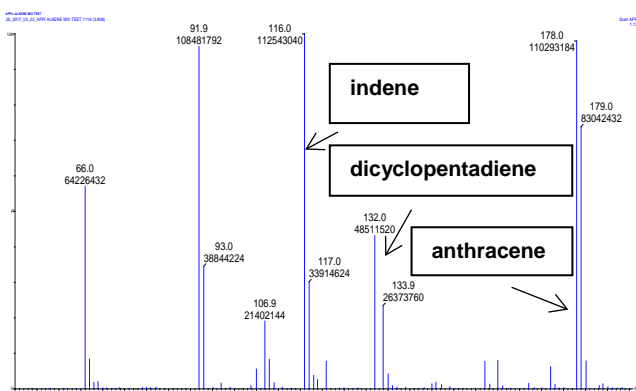


Figure 30 Positive ion APPI mass spectrum for a mixture of isoprene, indene, dicyclopentadiene and anthracene mixture.

The selectivity of diolefins and aromatic compounds by positive ion APPI MS negates the saturated hydrocarbon matrix of gasoline and simplifies the mass spectrum. Application of this technique to several deposit forming and non deposit forming fuels showed no correlation regarding deposit and

compound presence.

Port Fuel Injector (PFI) additives.

Polymeric gasoline additives can be identified as polyisobutene (PIB) or polypropylene glycol (PPG) by use of electrospray Fourier transform ion cyclotron mass spectrometry technique (ESI+ FT-ICRMS) and UHPSFC-ESI+ MS. Polymers can be identified by the characteristic spacing between the peaks within the ion series. The  $m/z$  values differing by the mass of the monomer units. Ionization additives can be used to manipulate the samples, enhancing ion intensity and simplifying the mass spectrum.

Different ionization techniques provide further information on the structure of the ions. Ionization by positive ion APPI indicates the presence of aromatic systems or conjugated double bonds within the molecule. Negative ion ESI indicates the presence of a site for deprotonating. The fuel used in injector 2 was found to have a PIB based deposit control additive (DCA) by these techniques (Figure 31).

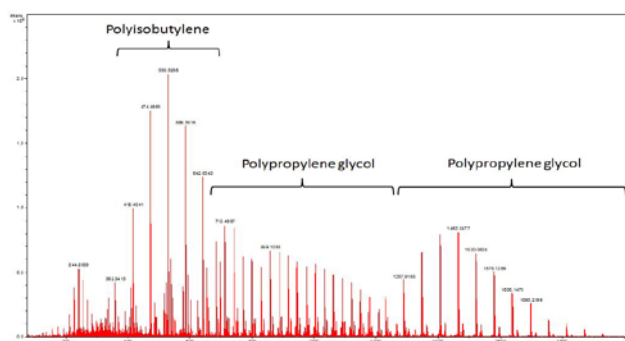


Figure 31 ESI+FT-ICR mass spectrum of fuel from injector 2

The degree of fouling on injector 2 when a DCA additive was present in the fuel indicated it was not mitigating deposit formation regarding the GDI injector. Therefore further work was undertaken to determine its end-group structure and thus understand its function in the fuel. A series of possible end group masses can be calculated *via* linear regression<sup>28</sup> using FT-ICRMS data. This corresponds to an elemental formula of C<sub>8</sub>H<sub>11</sub>NO (4.1 ppm error, 0.6 mDa). The termination of the polymerization of PIB results in one end group being a single hydrogen, so the other end group has an elemental formula of C<sub>8</sub>H<sub>10</sub>NO. This formula is consistent with a previously identified [29] PFI DCA additive (Figure 32).

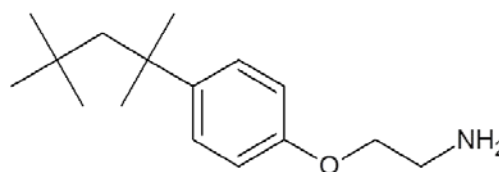


Figure 32 Proposed DCA structure

To determine the final structure tandem mass spectrometry/mass spectrometry (MS/MS) techniques were used to determine the end group structure in conjunction with accurate mass studies and deuterium exchange experiments. The accurate mass of the other ions common for all PIB molecules was investigated using the predominant  $m/z$  530 as an example (Figure 33).

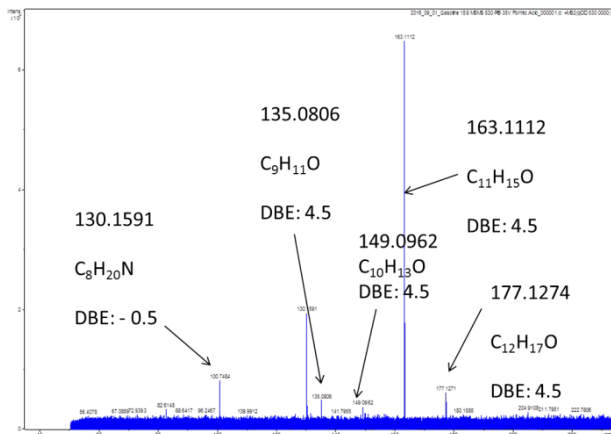


Figure 33 ESI+ FT-ICR MS product ion spectrum of  $m/z$  530.5300

The ion at  $m/z$  130.1591 (Figure 33) corresponds to an elemental formula of  $C_8H_{20}N$  (3.0 ppm error, 0.4 mDa), which are consistent with the protonated molecule of the corresponding neutral loss of  $m/z$  129.1515 loss from 530  $m/z$ . The remaining fragments within the positive ion ESI FT-ICR product ion mass spectrum are observed when fragmenting both  $m/z$  530 and  $m/z$  418, therefore are likely to originate from the polymer end group. The accurate mass measurement suggests these fragments contain an oxygen atom. The oxygen containing fragment ions each differ by a  $CH_2$  group, MS<sup>3</sup> of these ions identify that they are related, as  $m/z$  135, 149 and 163 can be obtained from the fragmentation of  $m/z$  177.

The ion at  $m/z$  130.1591 was further investigated by Tandem mass spectrometry using a third ion breakdown (MS<sup>3</sup>) utilizing the quadrupole ion trap (QIT). At low 1  $m/z$  resolution *i.e.*  $m/z$  130.  $m/z$  418 was fragmented at 40 % collision energy, resulting in  $m/z$  130, which was then isolated and fragmented at 25 % collision energy. The resulting product ion mass spectrum is presented, annotated with structural interpretations (Figure 34).

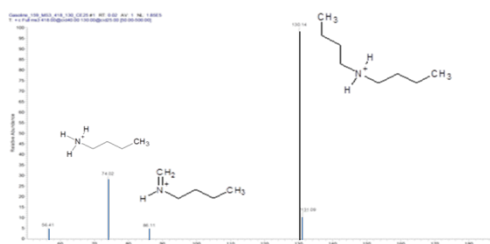


Figure 34. ESI+ QIT, MS2 product ion spectrum of  $m/z$

418 at 40 % collision energy, and then MS3 of  $m/z$  130 at 25 % collision energy

The fragmentation of  $m/z$  130 (figure 34) is characteristic of protonated di-butyl-amine. This is consistent with the accurate mass measurement for this ion. The neutral loss of 129  $m/z$  units from the protonated PIB molecule and the presence of the di-butyl amine at  $m/z$  130 suggests that DCA contains a di-butyl-amine pendant arm this is consistent with the structure of PIB Mannich deposit control additives (Figure 35).

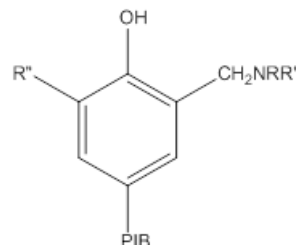


Figure 35 Generic structure of PIB-Mannich DCA

The above structure is associated with PFI additives and the amount of deposit on injector 2 shows the ineffectiveness of such technology with GDI technology.

## NEW GENERATION DCA GDI ADDITIVES

The work of Xu and Cracknell [35] has shown that for gasoline the injection system has a significant effect on PM emissions. Further clean injector condition and high inlet pressure are both required for low particle emissions.

Clearly there is an industry need for an effective GDI DCA additive. Innospec have recently launched Dynamico™ to service this need. This new GDI DCA is based on fundamentally different chemistries to that of traditional PFI DCAs. The following engine test data shows the results achievable.

## CLEAN UP

Testing was carried using Skoda engine – CAVE variant of VW EA111 engine, with the CEC-GDI cycle. Proposed CEC clean-up targets are 25% IPWI after 48 hour dirty-up run, 90% IPWI recovery after 24 hour clean-up. Tests on varying treat levels of additive formulations and different rates of clean-up performance were achievable.

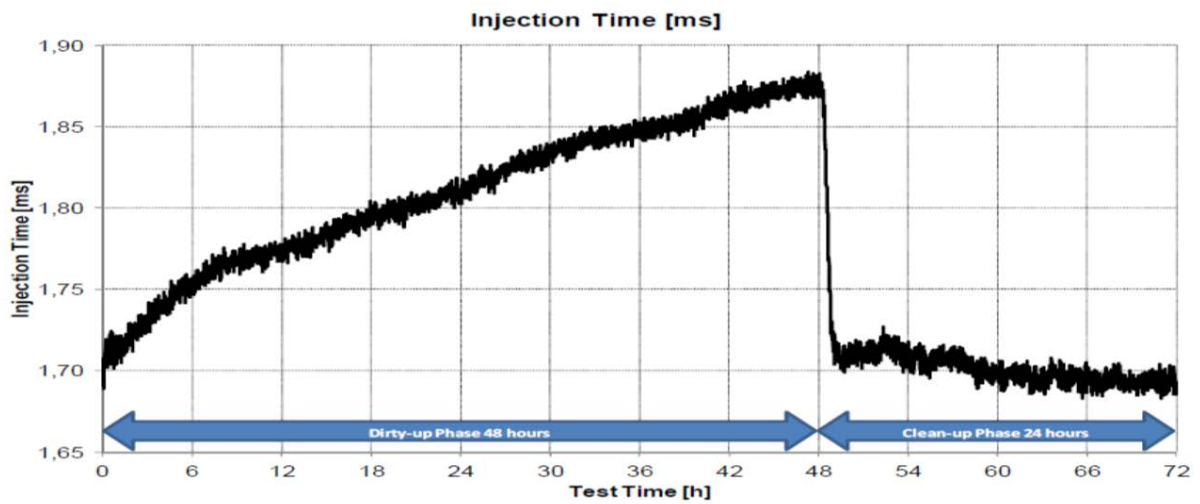
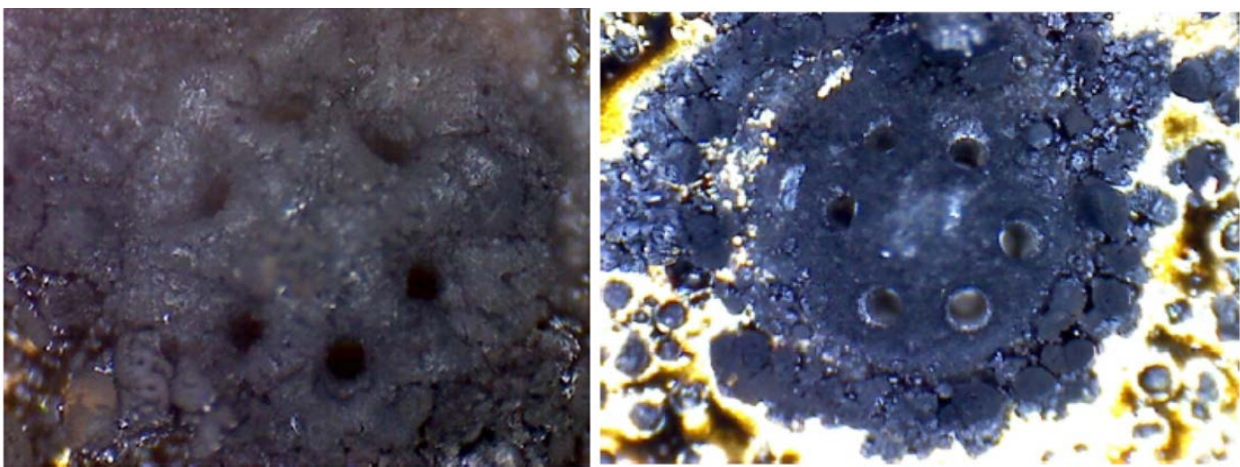


Figure 36 GDI testing –Clean Up

As the example in figure 36 shows 100% clean-up is achieved after one hour.



Base fuel

Additised fuel

Figure 37 Visual example of cleanup

The effectiveness is visually evident in figure 37.

### KEEP CLEAN

The ability to keep clean was also established for the new generation additive. Testing was undertaken using a Skoda engine equivalent to VW EA 111 engine. The proposed CEC clean up targets are 25% IPWI after 48 hour dirty-up run and 5% IPWI after 48 hour keep clean run.

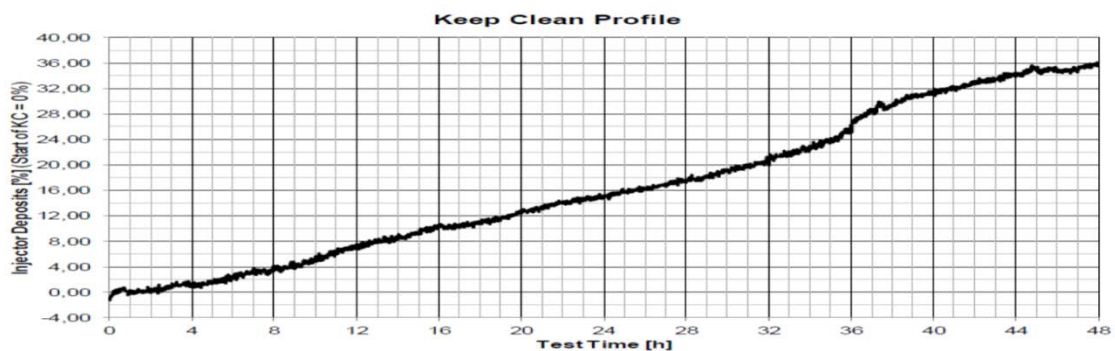


Figure 38 GDI testing keep clean basefuel

The results in Figure 38 for base fuel shows a change of injection time of 36.2% over 48hours.

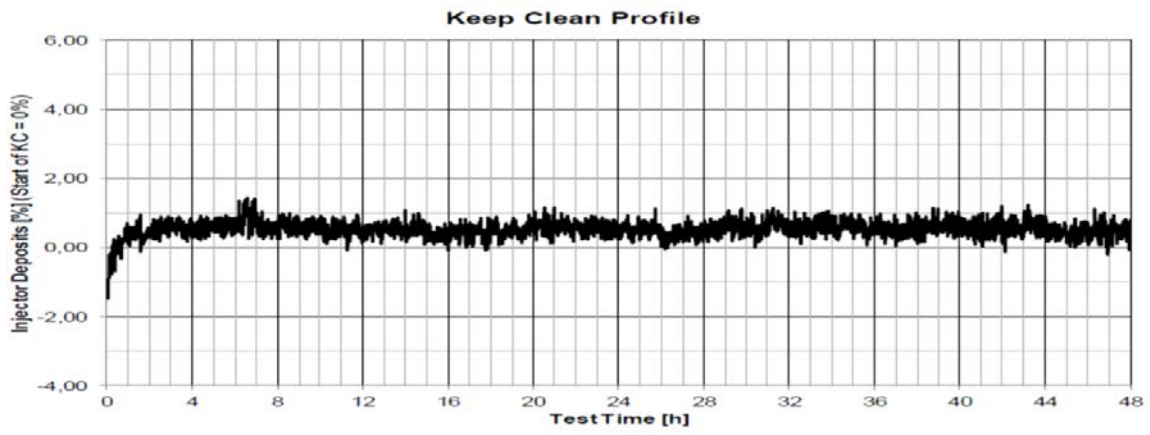


Figure 39 GDI testing keep-clean additized fuel

In the additized fuel test the change in injection time is 0.345%.

### PARTICLE EMISSIONS

The Vehicle test used a Mini Cooper S equipped with BMW B48 direct injection gasoline engine with turbocharger. Injector fouling tests were possible over relatively short test distances enabling the measurement of additive impact on particle number emissions

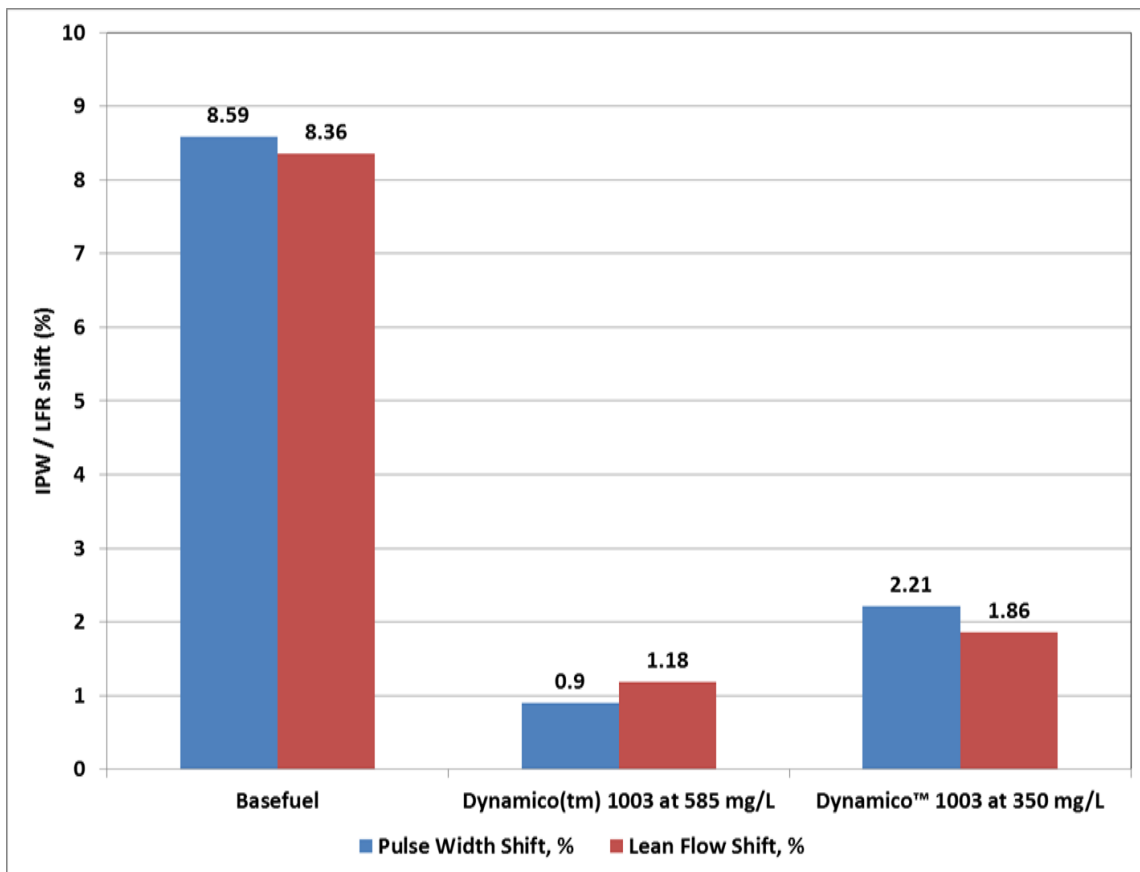


Figure 40 the demonstration of reduced injector fouling in a euro 6 vehicle with us of new generation GDI DCA additive.

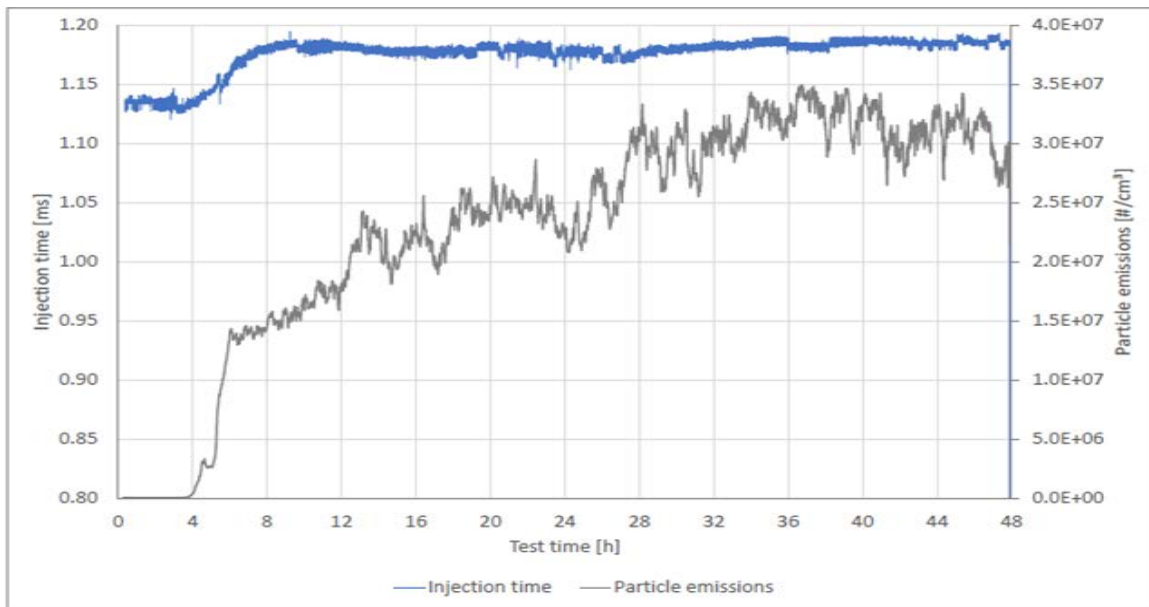


Figure 41 Increase in particle emission over length of test

During GDI testing, Particle emissions increase significantly over the test. At end of test particle emissions are 600 to 700 times higher (Figure 41).

As figure 42 shows, particle emissions can increase and can be 600 to 700 times higher at the end of the test. Addition of the new generation GDI DCA additive has a positive effect on reducing these emissions (figure 42). It will return a non-compliant vehicle to Euro 6 compliance in terms of PN emissions. Note the Euro 6 PN limit is  $6.0 \times 10^{11}$  #/Km.

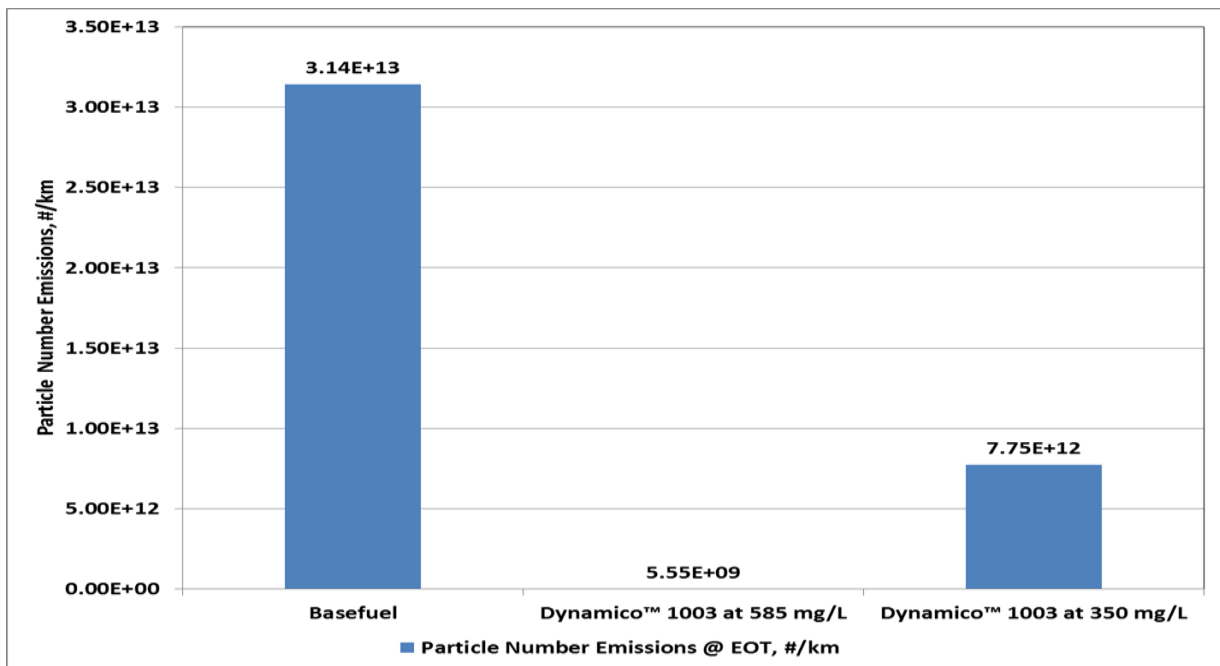


Figure 42 Effect of additization on PM emissions

The effectiveness of a new DCA in the removal of GDI deposits has been shown. The mechanism behind the build-up and removal of deposits with detergents is complex and not in the scope of this investigation. Detailed information on this subject can be found in the literature. [30-34].

## CONCLUSION

The characterization of GDI injector deposits may be carried out by a combination of SEM/EDS and FTIRM yielding data with regard to morphology, elemental make up and functionality.

Mass spectrometric characterization of the fuels that have produced these deposits has shown pro-deposit chemical species in the fuels and the presence of PFI DCA additives which have had little effect on the GDI nozzle deposit formation.

A new generation of GDI DCA additives not only allows control of GDI deposits and their removal and also reduces PN emissions.

## ACKNOWLEDGMENTS

The authors recognize the assistance of David Knight at Innospec for dismantling the injectors.

## REFERENCES

1. P. Richards, "Automotive Fuels Reference Book" 3<sup>rd</sup> Edition SAE 2014.
2. J. T. Marshall, "Direct injection For Wright Eighteen Cylinder Engine" *SAE Technical Paper* 480018 1948
3. G. Hartmann "Les moteurs et aéroplanes Antoinette" *Antoinette engines and aeroplanes*. <https://kimerius.com> accessed 16-04-2019
4. R van Basshuysen, "Ottomotoren mit Direkteinspritzung. Verfahren, Systeme Entwicklung, Potenzial", *Friedr. Vieweg & Sohn Verlag, GWV Fachverlage GmbH, Wiesbaden*. April 2007.
5. C. F. Taylor, E.S. Taylor and G.L. Williams "Fuel Injection with "Spark Ignition in an Otto cycle Engine," *SAE Technical Paper* 310005 1931.
6. S.E. Miller, "Automotive Gasoline Injection" *SAE Technical Paper* 560321 1956.
7. H. Manger, "Electronic Fuel Injection" *SAE Technical Paper* 820903 1982.
8. L.L. Bowler, "Throttle Body Fuel Injection (TBI)-An integrated Engine Control System," *SAE Technical Paper* 800164, 1980.
9. K. Takeda, K. Shiozawa, K. Oishi, and T. Inoue, "Toyota Central Injection (Ci) System for Lean Combustion and High Transient Response ", *SAE Technical Paper* 851675 1985.
10. J.R. Asik, D. A. Dobson and G.M. Meyer, "Suppression of Sulphide Emission During Lean Nox Trap Desulphurisation", *SAE Technical Paper* 2001-01-1299, 2001.
11. US Office of Energy Efficiency and Renewable Energy Fact #869, <https://www.energy.gov/eere/vehicles/fact-869>. Accessed 14-04-2019.
12. <https://www.theicct.org>. accessed 14004-2019
13. <http://www.easterncatalytic.com/education/tech-tips/fuel-trim-can-be-a-valuable-diagnostic-tool/>. Accessed 14-04-2019
14. <https://www.cectests.org>. Accessed 14-4-2019
15. <https://www.boschautoparts.com/en/auto/fuel-injectors/gasoline-direct-injection>; accessed: 28-08-2018
16. K Dearn, J. Xu, H. Ding, H. Xu et al, "An Investigation into the Characteristics of DISI Injector Deposits Using Advanced Analytical Methods" *SAE Int. J. Fuels Lubr.* 7(3): 2014, doi:10.4271/2014-01-272.
17. A. Berndorfer, S., Breur, W. Piock, P. von Bacho "Combustion Phenomena in GDi engines Caused by Injection Processes" *SAE Technical Paper* 2013-01-0261, 2013.
18. H. Xu, C. Wang, X. Ma, A. K. Sarangi, A. Weall, J. Krueger-Venus, "Fuel Injector Deposits in Direct-Injection Spark-Ignition Engines", *Prog. Energy Combust. Sci.*, 50, 63–80, 2015. DOI: 10.1016/j.pecs.2015.02.002
19. F. Pradelle, S. L. Braga, A. R. F. A. Martins, F. Turkovics, R. N. C. Pradelle, "Certainties and Challenges in Modeling Unwashed and Washed Gums Formation in Brazilian Gasoline–ethanol Blends", *Chem. Eng. Res. Des.*, 122, 77–96, 2017. DOI: 10.1016/j.cherd.2017.03.037
20. F. Pradelle, S. L. Braga, A. R. F. A. Martins, F. Turkovics, R. N. C. Pradelle, "Gum Formation in Gasoline and Its Blends: A Review", *Energy & Fuels*, 29 (12), 7753–7770, 2015 DOI: 10.1021/acs.energyfuels.5b01894
21. M. Kinoshita, A. Saito, S. Matsushita, H. Shibata, Y. Niwad, "Study of Deposit Formation Mechanism on Gasoline Injection Nozzle", *JSAE Rev*, 19(4), 355-357, 1998. DOI 10.1016/S0389-4304(98)00033-2
22. X. Zhang., G. Peng, G. Du, X. Sun, G. Jiang, X. Zeng P. Sun, B. Deng, H. Xie, Z. Wu, T. Xiao, "Investigating the Microstructures of Piston Carbon Deposits in a Large –Scale Marine Diesel Engine Using Synchrotron X-Ray Microtomography." *Fuel*, 142, 173-179, 2014.
23. S.S. Cheng "A micrographical Study of Deposit Formation Processes in a Combustion Chamber " *SAE technical Paper* 962008. 1996.
24. G.M. Reed, R. Wilson, R. Juskaitis, M.A.A. Neil, "Surface Profiling of Combustion Chamber Deposits Using Aperture Correlation Confocal Microscopy." *J. Microsc.* 189(3) 188-191, 1998.
25. W. M. Studzinski, J.M. Cummings, "Reference Fuel Composition". *US8764854 B1*, 2014
26. F. Pradelle, S. Braga, A.R.F.A. Martins, F. Turkovics, R.N.C.; Pradelle, "Gum Formation in Gasoline and Its Blends: A Review". *Energy Fuel*, 29, (12), 7753-7770, 2015.
27. I. Di Somma, R. Marotta, R.; Andreatti, V. Caprio, "Dicumyl Peroxide Thermal Decomposition in Cumene: Development of a Kinetic Model". *Ind Eng, Chem. Res.*, 51, (22), 7493-7499 2012.
28. S. Koster, M.C.; Dursma, J.J.; Boon, R.M.A. Heeren, "Endgroup Determination of Synthetic Polymers by Electrospray Ionization Fourier Transform Ion Cyclotron Resonance Mass Spectrometry." *J. Am. Soc. Mass Spectr.* 11, (6), 536-543 2000
29. T/ Lynch, S Whitmarsh, C.; Wicking, "In Selective Ionisation With High Resolution Mass

*Spectrometry - The Future for Hyphenation in the Petrochemical Industry?"* HTC-14, Ghent, Belgium; Ghent, Belgium, 2016

30. A. Aradi, W. Colucci, H. Scull and M. Openshaw, "A Study of Fuel Additives for Direct Injection Gasoline (DIG) Injector Deposit Control," *SAE Technical Paper* 2000-01-2020, 2000, doi:10.4271/2000-01-2020.
31. A. Aradi, J. Evans, K. Miller, A. and Hotchkiss, "Direct Injection Gasoline (DIG) Injector Deposit Control with Additives," *SAE Technical Paper* 2003-01-2024, 2003, doi:10.4271/2003-01-2024.
32. A. Joedicke, J. Krueger-Venus, P. Bohr, R. Cracknell, et al., "Understanding the Effect of DISI Injector Deposits on Vehicle Performance," *SAE Technical Paper* 2012-01-0391, 2012, doi:10.4271/2012-01-0391.
33. D. Arters and M. Macduff, "The Effect on Vehicle Performance of Injector Deposits in a Direct Injection Gasoline Engine," *SAE Technical Paper* 2000-01-2021, 2000, doi:10.4271/2000-01-2021.
34. A. Prakash, E. Nelson, A. Jones, J. Macias, et al., "Particulate Mass Reduction and Clean-up of DISI Injector Deposits via Novel Fuels Additive Technology," *SAE Technical Paper* 2014-01-2847, 2014, doi:10.4271/2014-01-2847.
35. C. Wang H. Xu J. Herreros J. Wang R. Cracknell "Impact of Fuel and Injection and Injection Systems on Particle Emissions from a GDI engine" *Applied Energy* 132,178-191 2014. <https://doi.org/10.1016/j.apenergy.2014.06.012>.

## CONTACT

James Barker

Tel: +44 151 355 3611

Email: [jim.barker@innospecinc.com](mailto:jim.barker@innospecinc.com)

Innospec Limited  
Innospec Manufacturing Park  
Oil Sites Road, Ellesmere Port  
Cheshire  
CH65 4EY  
England  
<http://www.innospecinc.com>

